



**HAL**  
open science

## Reproduction of Geogrid In Situ Damage Used in Asphalt Concrete Pavement with Indentation Tests

Cyrille Chazallon, Cédric Barazzutti, Hervé Pelletier, Mai-Lan Nguyen, Pierre Hornych, Saïda Mouhoubi, Daniel Doligez

► **To cite this version:**

Cyrille Chazallon, Cédric Barazzutti, Hervé Pelletier, Mai-Lan Nguyen, Pierre Hornych, et al.. Reproduction of Geogrid In Situ Damage Used in Asphalt Concrete Pavement with Indentation Tests. Journal of Testing and Evaluation, 2019, 48 (1), pp.20180929. 10.1520/JTE20180929 . hal-03083248

**HAL Id: hal-03083248**


**<https://hal.science/hal-03083248>**

Submitted on 2 Jan 2024

**HAL** is a multi-disciplinary open access archive for the deposit and dissemination of scientific research documents, whether they are published or not. The documents may come from teaching and research institutions in France or abroad, or from public or private research centers.

L'archive ouverte pluridisciplinaire **HAL**, est destinée au dépôt et à la diffusion de documents scientifiques de niveau recherche, publiés ou non, émanant des établissements d'enseignement et de recherche français ou étrangers, des laboratoires publics ou privés.

# AUTHOR QUERY FORM









 ASTM INTERNATIONAL	Journal: J. Test. Eval.  Article Number: JTE20180929	Please provide your responses and any corrections by annotating this PDF and uploading it to ASTM's eProof website as detailed in the Welcome email.
---	--	--

Dear Author,








Below are the queries associated with your article; please answer all of these queries before sending the proof back to ASTM Production. Please contact ASTM at [astmproduction@jeditorial.com](mailto:astmproduction@jeditorial.com) with any questions or concerns.

1. Please ensure accuracy of all affiliations, ORCID information, and spelling of all authors' names.
2. Please confirm corresponding author's email address and indicate if it has changed since submission. Note: only the corresponding author's email address will be included in the article.
3. Please review all tables and/or equations for accuracy.
4. Please thoroughly review all figures. If necessary, revised figures can be sent along with page proof corrections. Digital files can be attached to your annotated PDF.
5. Please provide email addresses for all authors. Complimentary PDFs of the final article will only be provided to authors with a valid email address. Please note that only the corresponding author's email address will be published.

Please respond to the following queries by clicking on the **AQ** link and inserting your comments or corrections as a PDF annotation. Additional comments can be left in the **Author Comments** column. We may require your response in order to proceed with production; unanswered queries may cause delays in publication.

Location in article	Query/Remark	Author Comments
<a href="#">AQ1</a>	AQ: Please expand the following abbreviations appearing in the affiliations: UMR, CNRS, INSA, and IFSTTAR.	
<a href="#">AQ2</a>	AQ: Please ensure that department/division information has been provided for each author affiliation.	
<a href="#">AQ3</a>	AQ: Please ensure that a full mailing address has been provided for each author affiliation (this includes a full street address).	
<a href="#">AQ4</a>	AQ: Please define the abbreviation "AC" upon first use in the text.	
<a href="#">AQ5</a>	AQ: Please expand the abbreviation "ESEM."	
<a href="#">AQ6</a>	AQ: We note that Ref. 4 could not be verified. Please check and confirm that the information contained in the reference is correct and accurate.	
<a href="#">AQ7</a>	AQ: Please provide the full approval date for the ASTM standard cited in Ref. 7.	
<a href="#">AQ8</a>	AQ: We note that Ref. 11 could not be verified. Please check and confirm that the information contained in the reference is correct and accurate.	

Please confirm the following revisions by clicking on the **C** link and reviewing the revision. If you do not approve the change, please leave a comment or correction as a PDF annotation. Additional comments can be left in the **Author Comments** column. If you do not respond to the query, the change will be approved.

<b>Location in article</b>	<b>Query/Remark</b>	<b>Author Comments</b>
<a href="#">C1</a>	C: In the sentence beginning “When we perform a bibliographic study...,” we have changed “Khodaii, Fallah, Nejad” to “Khodaii and Fallah.” Please review and confirm whether this is correct.	
<a href="#">C2</a>	C: The sentence beginning “When we perform a bibliographic study...” has been edited for clarity. Please review and confirm whether the sentence is correct.	
<a href="#">C3</a>	C: The sentence beginning “The tests consisted in building test sections...” has been edited for clarity. Please review and confirm whether the sentence is correct.	
<a href="#">C4</a>	C: We have defined the abbreviation “SCAC” as “self-compacting asphalt concrete.” Please review and confirm whether this is correct.	
<a href="#">C5</a>	C: In the sentence beginning “In total, five test sections were...,” we have expanded the abbreviation “FWD” as “falling weight deflectometer.” Please review and confirm whether this is correct.	
<a href="#">C6</a>	C: The sentence beginning “The grids could be so affected by three types...” as well as the sentence immediately following it have been edited for clarity. Please review and confirm whether the sentence is correct.	
<a href="#">C7</a>	C: The sentence beginning “The resistance to penetration measured by indentation...” has been edited for clarity. Please review and confirm whether the sentence is correct.	



**Complete this quote request and return by:**  
Email [service@astm.org](mailto:service@astm.org)  
Fax +1.610.832.9555  
Mail  
ASTM International  
Attention: Inside Sales and Service  
100 Barr Harbor Drive, PO Box C700  
West Conshohocken, PA 19428-2959

# Reprints Order Form

For reprints of articles and/or papers from *ASTM Journals*, *Selected Technical Papers (STPs)*, book chapters, and *Standardization News*

*Authors receive a 25% discount*

Ship to:

Name	<input type="text"/>		
Organization	<input type="text"/>		
Address	<input type="text"/>		
City	State	Zip	<input type="text"/>
Country	<input type="text"/>		

Bill to:

Name	<input type="text"/>		
Organization	<input type="text"/>		
Address	<input type="text"/>		
City	State	Zip	<input type="text"/>
Country	<input type="text"/>		

Reprint requesting:

Paper Title	<input type="text"/>		
Publication (title, month, and volume, STP, or stock number)	<input type="text"/>		
Page length of article	<input type="text"/>	Number of copies (25 minimum)	<input type="text"/>
Cover (check one)			
<input type="checkbox"/> Reprinted article, no cover	<input type="checkbox"/> Reprinted article and cover with typeset title of article and author's name		

Date	Tel	Email	Fax	<input type="text"/>
------	-----	-------	-----	----------------------

**For order questions, please contact ASTM Inside Sales and Service**  
[service@astm.org](mailto:service@astm.org) | tel +1.610.832.9585 | [www.astm.org](http://www.astm.org)



# Reprints Price Scale

(Prices subject to change without notice)

## Color Reprints

Pages/Copies	100	200	500	1,000	2,000
2	\$1,102	\$1,323	\$1,543	\$1,764	\$1,984
3-4	\$2,116	\$2,221	\$2,326	\$2,425	\$2,824
5-8	\$2,168	\$2,278	\$2,394	\$2,499	\$3,024
9-12	\$3,307	\$3,470	\$3,638	\$3,801	\$4,126

## Black & White Reprints

Pages/Copies	25	50	100	200	300	500	1,000	2,000
1-4	\$136	\$152	\$168	\$184	\$199	\$226	\$310	\$472
5-8	\$195	\$226	\$257	\$278	\$299	\$352	\$499	\$709
9-12	\$225	\$257	\$289	\$336	\$357	\$425	\$577	\$787
13-16	\$263	\$294	\$325	\$394	\$430	\$520	\$751	\$1,118
17-20	\$278	\$336	\$394	\$472	\$514	\$635	\$887	\$1,307
21-24	\$301	\$373	\$446	\$535	\$583	\$724	\$1,003	\$1,475
25-28	\$331	\$404	\$478	\$583	\$646	\$808	\$1,165	\$1,795
29-32	\$383	\$441	\$299	\$651	\$724	\$913	\$1,323	\$2,058
Cover (optional)	\$100	\$115	\$136	\$157	\$178	\$220	\$373	\$598

ASTM International Inside Sales and Support department will contact you with a final price quote, including freight charges,

**For order questions, please contact ASTM Inside Sales and Service**  
 service@astm.org | tel +1.610.832.9585 | www.astm.org



## Journal of Testing and Evaluation

---

Cyrille Chazallon,<sup>1</sup> Cédric Barazzutti,<sup>2</sup> Hervé Pelletier,<sup>2</sup> Mai-Lan Nguyen,<sup>3</sup>  
Pierre Hornych,<sup>3</sup> Saida Mouhoubi,<sup>4</sup> and Daniel Doligez<sup>5</sup>

**DOI: 10.1520/JTE20180929**

### Reproduction of Geogrid In Situ Damage Used in Asphalt Concrete Pavement with Indentation Tests

---

Cyrille Chazallon,<sup>1</sup> Cédric Barazzutti,<sup>2</sup> Hervé Pelletier,<sup>2</sup> Mai-Lan Nguyen,<sup>3</sup>  
Pierre Hornych,<sup>3</sup> Saida Mouhoubi,<sup>4</sup> and Daniel Doligez<sup>5</sup>

## Reproduction of Geogrid In Situ Damage Used in Asphalt Concrete Pavement with Indentation Tests

### Reference

C. Chazallon, C. Barazzutti, H. Pelletier, M.-L. Nguyen, P. Hornych, S. Mouhoubi, and D. Doligez, "Reproduction of Geogrid In Situ Damage Used in Asphalt Concrete Pavement with Indentation Tests," *Journal of Testing and Evaluation* <https://doi.org/10.1520/JTE20180929>

### ABSTRACT

Geogrids are used for the rehabilitation of cracked pavements. To ensure an efficient reinforcement, it is required to know the residual mechanical properties of the geogrid after its implementation and compaction of the above asphalt concrete layer and the level of damage of the grid. This article presents the results of the national French project SolDuGri dealing with pavement reinforcement by geogrids and more precisely the reproduction in laboratory of the in situ damage. In this project, full-scale tests have been performed to evaluate the in situ damage of four different types of geogrids in asphalt concrete pavements. Then, after construction, the geogrids have been recovered from different locations on the field sections, where they had been subjected to compaction. These grids have been subjected to direct tension tests in the laboratory. Laboratory analyses like scanned asphalt concrete and geogrid surfaces have been performed to evaluate indenter shapes. Different sets of indenters have been made, and a laboratory complete study of geogrid indentation tests has been performed with different sets of temperature, indenter shapes, and indentation forces. The first conclusions are that the indenter geometry and the temperature have the main influence on the strength resistance and elastic modulus of the grid. Results obtained after indentation performed in laboratory can be compared to those measured on in situ recovered grids.

### Keywords

glass fiber grids, indentation test, direct tension test

Manuscript received December 14, 2018; accepted for publication July 23, 2019; published online xxxx xx, xxxx.

<sup>1</sup> Shandong Provincial Key Laboratory of Road and Traffic Engineering in Colleges and Universities, Shandong Jianzhu University, Fengming Rd., Lingang Development Zone, 250101 Jinan, China; and ICube UMR7357, CNRS, INSA de Strasbourg, Université de Strasbourg, de 24 Blvd. de la Victoire, 67084 Strasbourg CEDEX, France (Corresponding author), e-mail: [cyrille.chazallon@insa-strasbourg.fr](mailto:cyrille.chazallon@insa-strasbourg.fr), <https://orcid.org/0000-0002-0993-5019>

<sup>2</sup> Institut Charles Sadron, UPR22, CNRS, INSA de Strasbourg, Université de Strasbourg, 23 Rue du Loess, 67200 Strasbourg, France

<sup>3</sup> IFSTTAR, Centre de Nantes, Route de Bouaye, CS4, 44344 Bouguenais CEDEX, France

<sup>4</sup> ICube UMR7357, CNRS, INSA de Strasbourg, Université de Strasbourg, de 24 Blvd. de la Victoire, 67084 Strasbourg CEDEX, France

<sup>5</sup> 6D Solutions, 17 Place Xavier Ricard, 69110 Sainte Foy lès Lyon, France

## Introduction

Geogrids are generally used for the rehabilitation of cracked pavements (semirigid pavements, asphalt pavements, and flexible pavements), but nowadays, they are also included in new pavements. To ensure an efficient reinforcement and a reliable design of the pavement incorporating a grid, it is required to know the residual mechanical properties of the geogrid after its implementation and compaction of the above asphalt concrete layer and the level of damage of the grid.

When we perform a bibliographic study on asphalt concrete reinforced by grids, one can observe that the damage of the grid is not taken into account in the modellings that are performed either analytically or with finite element methods, as shown in Graziani et al.<sup>1</sup> and Khodaii and Fallah.<sup>2</sup> Recently some studies from a field test or laboratory compaction test underline that multiple damage exist, which are revealed in the analysis of the tensile strength and of the stiffness of the recovered grids, as shown in Gonzalez-Torre et al.,<sup>3</sup> van Rompu et al.,<sup>4</sup> Chazallon et al.,<sup>5</sup> and Chazallon et al.<sup>6</sup> This damage depends on the hardness of the coating and the shape of the yarns. Nowadays, the main grids that are used for pavement reinforcement are cost-effective grids made of glass fibers. If coated glass fiber grids are subjected to less damage than the uncoated ones, it is crucial to be able first to quantify their damage level in strength and stiffness and then to know how to reproduce it with laboratory conditions in order to improve the grids design: coating and shape of the yarns.

This article presents the results of the national French project SolDuGri dealing with pavement reinforcement by geogrids and more precisely the reproduction in laboratory of the in situ damage concerning the mechanical strength and the stiffness modulus. In this project, full-scale tests have been performed to evaluate the in situ damage of geogrids in asphalt concrete pavements. The tests consisted in building test sections with four different types of geogrids and two different compacted asphalt concrete layers located above the geogrids. After construction, the geogrids have been recovered from different locations on the field sections, where they had been subjected to compaction only, or also to construction traffic, and their residual mechanical properties have been evaluated in the laboratory. We will present the materials used, the tested sections, and then the tensile tests on recovered grids. In parallel, we try to reproduce in the laboratory the damage observed on in situ recovered grid using a modified experimental indentation setup. For this, we present the first results of laboratory indentation tests using specific indenters whose geometries have been determined from asphalt concrete surface shapes in contact with the grids. To estimate the loss after damage by indentation, the experimental data deduced from ultimate tensile tests using ASTM D 6637/D 6637M, *Standard Test Method for Determining Tensile Properties of Geogrids by the Single or Multi-Rib Tensile Method*,<sup>7</sup> were compared to results obtained on new grids without any damage.<sup>6</sup> We can notice that the mechanical properties are affected by the indentation effect, especially the resistance strength that is slightly reduced.

## Materials Used

### SEMICOARSE ASPHALT CONCRETE MATERIAL

For this test, the asphalt concrete material chosen is a standard semicoarse asphalt concrete (self-compacting asphalt concrete [SCAC] “AC 10 surf 35/50” according to NF EN 13108-1, *Mélanges bitumineux - Spécifications des matériaux - Partie 1 : enrobés bitumineux*<sup>8</sup>) designed with the crushed aggregates in the area where the experimentation was to be carried out. The binder is a 35/50 penetration grade bitumen according to NF EN 12591, *Bitumes et liants bitumineux - Spécifications des bitumes routiers*.<sup>9</sup> The stiffness modulus, measured by two-points bending tests, is 12,945 MPa at 15°C and 10 Hz for the hot mix (160°C).

These asphalt concretes have been used in their usual range of thickness: 5 to 7 cm. The tack coat between the asphalt layers, including the grid impregnation, was a classical cationic rapid setting bitumen emulsion, classified as C69B3 according to NF EN 13808, *Bitumes et liants bitumineux - Cadre de spécifications pour les émulsions cationiques de liants bitumineux*.<sup>10</sup>



## GLASS FIBER GRIDS

Four different grids, made of glass fiber coated with two different resins, of different hardness, were chosen for the study. The first two grids (G1 and G2) had a strength of 20 kN/m for a strain of 1 % and were coated with a stiff resin and a soft resin, respectively. The two other grids (G3 and G4) had a 40 kN/m strength at 1 % strain, stiff and soft resins, respectively.

## Tested Sections

In total, five test sections were built for the SolDuGri project on an existing subgrade with a load-bearing capacity higher than 100 MPa (falling weight deflectometer tests). One of these sections, 15 m long, was devoted to the study of grid damage after construction. This section included the four different types of geogrids (G1, G3, G2, and G4).

A leveled asphalt concrete layer was firstly realized on the existing subgrade. Four SCAC layers, each 5 cm thick, were then laid one after the other to constitute the pavement test section (fig. 1).

The 20-cm-thick pavement structure was chosen because a thick structure was required for other laboratory studies planned in the SolDuGri project.<sup>11</sup> Void content measurements by a Troxler device on the surface of the second and fourth layers indicated mean void contents of 5.7 % and 5.8 %, respectively, on sections made of hot mix.

The different geogrids were placed on the surface of the second SCAC layer. To study the effect of different surface conditions on the damage of the geogrids, on one half of the section, the surface of the second SCAC layer was milled before placing the grids (to simulate the reinforcement of an old pavement—surface B), and the second part was compacted normally to simulate a new construction (surface A). On both parts, a tack coat with 500 g/m<sup>2</sup> of residual bitumen was applied to ensure impregnation of the geogrids. A tack coat with 300 g/m<sup>2</sup> of residual bitumen was applied on the other interfaces. The full-scale test sections were built using standard roadwork equipment (fig. 2) as used on real construction sites. The grids could be so affected by three types of impact during the construction: movements of pneumatic tires of delivery trucks and movements of metallic caterpillars of paving machines directly on some grids, as well as the indentation of aggregates because of the compaction on the whole surface of grids. The positions of traffic, i.e., truck tires and metallic caterpillars of paving machines, on the pavement during each phase of construction were precisely measured and reported for the investigation.

For the study of the geogrid damage after construction, a specific procedure of placement of the geogrids was adopted. The four different types of grids were cut in small sections, 72 cm by 72 cm large. After construction, when the pavement was completely cooled, the geogrids were recovered from different locations on the field sections, where they had been subjected to compaction only, or also to construction traffic, by the trucks and by the finisher. Care was taken to minimize the damage of the grids during recovery. Each grid section

**FIG. 1**

Transverse profile of test sections.

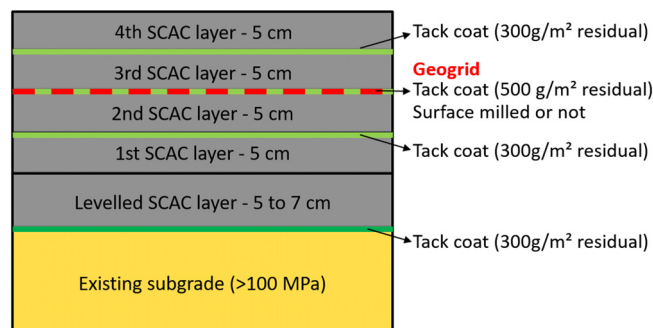


**FIG. 2** Construction of the full-scale test sections and trafficking of construction equipment on the grids.

was located and sawed in a block of about 64 by 64 cm<sup>2</sup>. Each block was then placed inside a large oven and heated 107  
to 40°C for about 5 to 7 h. The recovered geogrid sections were finally marked to identify their type and their 108  
location on the field section, and they were sent to the laboratory for evaluation of their residual mechanical 109  
properties. 110

Although great care was taken for the recovering of the geogrid sections, 100 % of the yarns could not be 111  
recovered properly without any damage because of the strong bond between the geogrids and the asphalt concrete 112  
layers. After a visual examination, all the grids that have yarns that were cut or seemed to have been torn or bent 113  
during the extraction were eliminated. Only grids that had been damaged directly by the pavement construction 114  
process were considered for laboratory evaluation. 115

## Tension Tests on Recovered Grids 116

In total, 32 grid sections were placed in the test section and have been recovered. A total of 27 have been tested 117  
until now. Each section was trafficked on more than 50 % of its surface by the wheels of the delivery trucks or the 118  
metallic caterpillars of the finisher while paving the test section. Concerning the tension tests, slightly less than 119  
50 % of the yarns had been damaged only by the compaction, although a little more than 50 % had been damaged 120  
by both compaction and trafficking by the caterpillars or the wheels. 121

During recovery, the loading received by each grid was carefully identified (see [Table 1](#)), and three different 122  
loading processes were distinguished: 123

- Grids submitted only to compaction of the upper layers without any other loading (no loading). 124
- Grids submitted to compaction and to loading by the wheels of the asphalt truck (tire). 125
- Grids submitted to compaction and loading by the finisher's caterpillars. Because of the narrow asphalt 126  
layers, a small finisher with an overall width of the caterpillars of 1.5 m was used. This width was smaller 127  
than the spacing of the truck wheels. Therefore, the zones loaded by the caterpillars were different from the 128  
zones loaded by the tires. 129

**TABLE 1**

Number of warp and filling yarns tested per loading type and per support type (A/B)

Grid	G1 (A/B)	G2 (A/B)	G3 (A/B)	G4 (A/B)
No loading (NL)	51 (32/19)	29 (16/13)	31 (4/27)	25 (4/21)
Tires (T)	51 (27/24)	35 (17/18)	45 (14/31)	35 (12/23)
Caterpillars (C)	21 (7/14)	10 (5/5)	21 (4/17)	7 (0/7)

Each recovered grid was cut into individual warp or filling yarns, which were submitted to tension tests. The yarn samples were 29 cm long and were tested at 20°C. For each yarn, the secant modulus was determined between the maximum force and 100 N (small strain tests were also performed). The strains were measured with the press strain measurement device and a local extensometer for the small strain tests. The same tests have also been performed on new grids coming from the manufacturer for comparison.<sup>5,12</sup>

Globally, after 361 traction tests, these tests give the following results: one observes residual strengths varying between 20 and 55 % of initial tensile strengths and residual secant moduli at the maximum strength between 68 and 95 % of initial secant moduli at the maximum strength.<sup>6</sup>

## Reproduction of In Situ Damage of Geogrids

In order to reproduce in the laboratory the damage observed on recovered geogrid by compaction and trafficking, the first step has consisted in the accurate analysis of the topography of real asphalt concrete blocks coming from in situ test sections using numerical microscopy (HIROX RH 2000), as described in [figure 3A](#).

The surface (15 by 15 cm<sup>2</sup>) of each asphalt concrete block that has been in contact with the geogrid has been observed. These asphalt concrete blocks have been extracted from hot mixed asphalt concrete slabs compacted in the laboratory with the same AC 10 surf 35/50 (same density, binder, aggregates), which were used for the in situ test section. By analyzing several cross profiles in two in-plane directions (see in [fig. 3A](#) bottom), specific peaks associated with surface asperities have been identified and then geometrically characterized (shape, characteristic lengths such as height, edge length, edge radius, opening angle). Two specific peak geometries are involved for each block surface: conical and V shaped.

[Figure 3B](#) shows the evolution of the measured open angle as a function of the measured curvature radius for the block whose surface topography is depicted in [figure 3A](#). From these experimental data, a statistical analysis has been performed for eight real concrete blocks, as depicted in [figure 3C](#) for the measured open angle. Two average values can be extracted from statistical analysis: average values of open angle close to 110° and of radius of curvature of 0.7 mm. From these two average values, a wide range of conical and V-shaped indenters have then been designed. About 45 indenter geometries have been manufactured with open angles varying from 90° to 130°, two values of tip radius less than 0.1 and 0.7 mm, and for V-shaped indenters, with edge lengths varying between 1 and 14 mm, as depicted in [figure 4](#). After machining, each indenter tip has been controlled using numerical microscope observations ([fig. 4B](#) and [4C](#)). The material used for indenters is a hardened nickel-chromium steel to avoid or limit their plastic deformation during indentation tests.

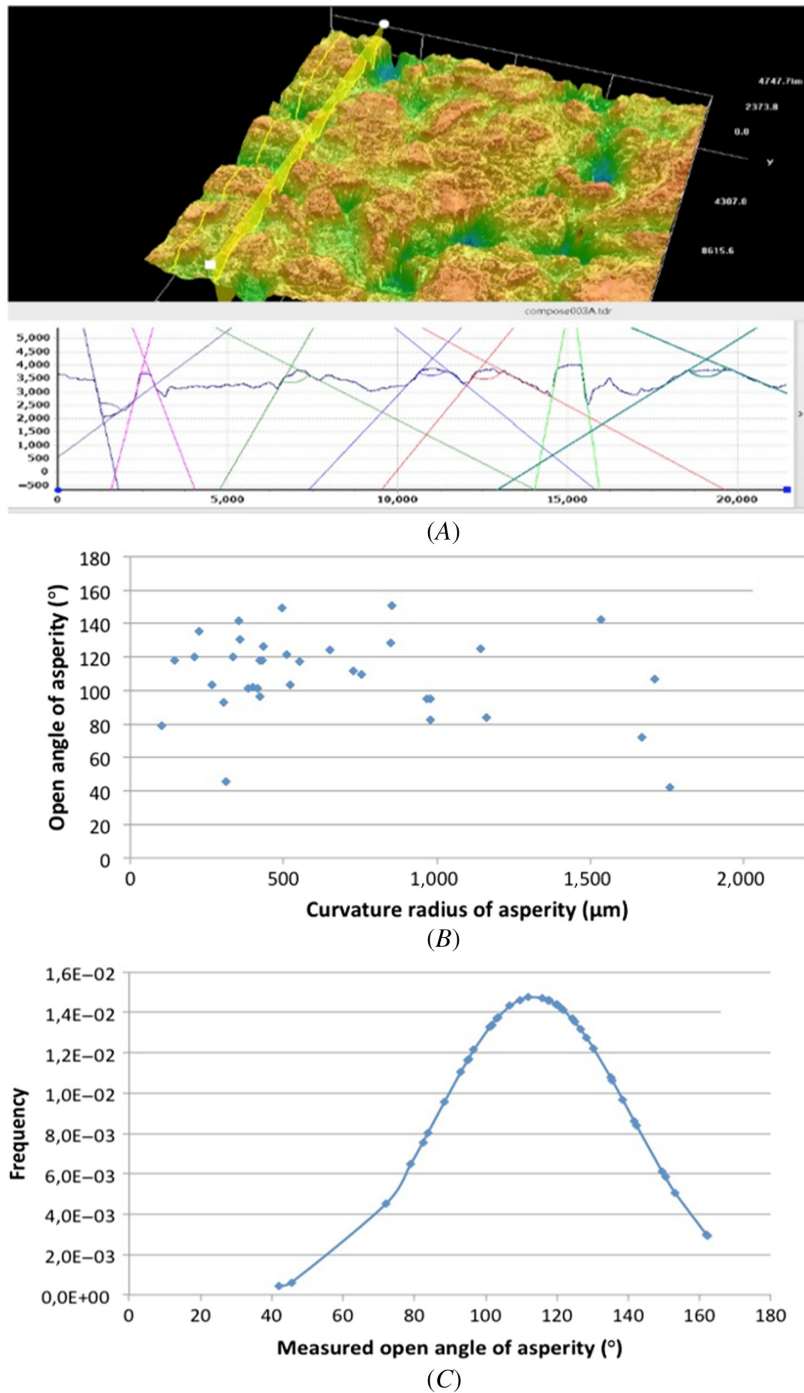
To realize indentation tests, an universal Bruker's UMT Tribolab experimental setup has been equipped with built-in sample holders to fix the tested geogrid yarns ([fig. 5](#)). Two options are integrated to this sample holder: (i) a heating system to perform indentation tests both at room temperature and also at 100°C (±5°C), and (ii) a specific plate in order to control the orientation of the geogrid during indentation tests, especially when using V-shaped indenters.

For all indentation tests, the indenter tip is pushed in contact to the surface of the geogrid yarns. An initial preload of 2 N is applied, and then a linear increasing load is imposed up to a maximal value of 900 N at a loading rate of 20 N · s<sup>-1</sup>. After a holding time of 5 s, the load is linearly decreased from 900 to 0 N at an unloading rate of 20 N · s<sup>-1</sup>. For each of the testing conditions and for each sample, indentation experiments have been replicated three or five times as a function of the observed experimental scattering. Because of the stiffness of the experimental setup, the measured penetration depth has to be corrected as a function of the normal applied load ( $F_z$ ). The determination of the stiffness is a standard procedure for load and displacement-sensing indentation experiments. Indentation tests are performed by increasing progressively the normal load applied in a hard sample, whose mechanical properties are well known.<sup>13</sup>

[Figure 6](#) exhibits experimental load-displacement curves obtained as a function of indenter geometries and the tested temperature for a given grid (the penetration depth ratio [pdr] corresponds to the ratio between the effective penetration depth and the real thickness of the tested yarn). It is interesting to note the characteristic

**FIG. 3**

Three-dimensional surface topography obtained by numeric microscope HIROX of a real concrete asphalt block (A) and corresponding statistical analysis showing the evolution of the open angle as a function of the curvature radius (B) and the distribution of measured open angle of asperities (C).



curve describing the applied load as a function of the penetration depth that does not follow a classical kick's law 176  
 $(F_z = C \cdot h^2)$ , with  $F_z$ , the normal applied load,  $h$ , the effective penetration depth, and  $C$ , a constant function of the 177  
indenter tip geometry and the hardness of the tested material), especially at room temperature. For shallow in- 178  
indentation depth, the tip penetrates rapidly into the grid (with a horizontal slope), and at a specific penetration 179



**FIG. 4** Examples of V-shaped indenters with an edge length of 10 mm with different open angles manufactured in hardened nickel-chromium steel (A). Projected profiles of conical (B) and V-shaped (C) indenters measured using a numerical microscope in order to control their geometrical properties after machining.

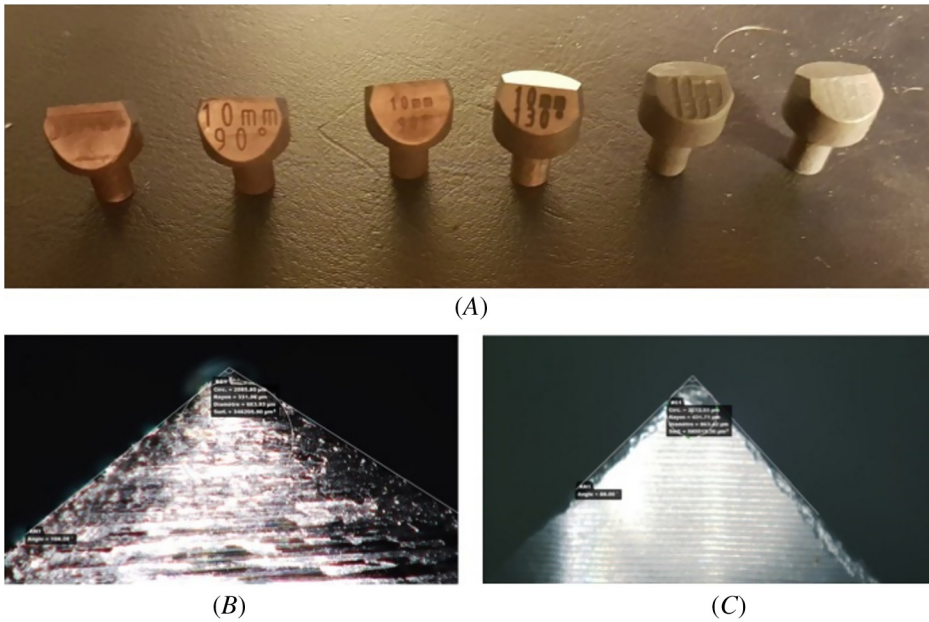
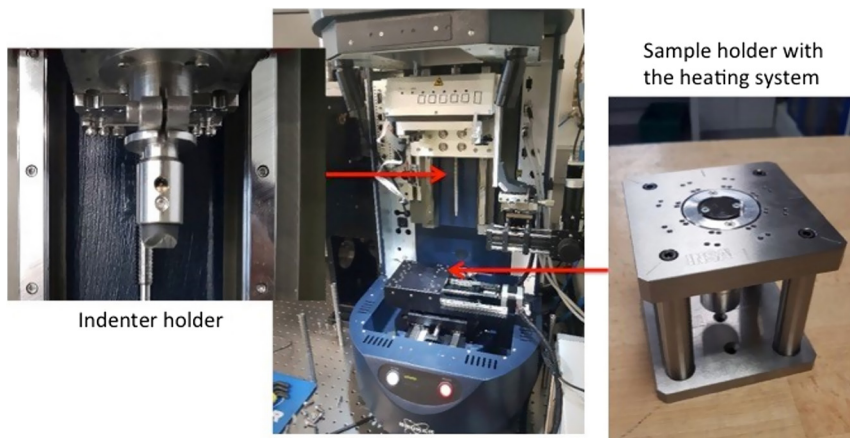


**FIG. 5** Experimental indentation setup (UMT Tribolab, Bruker) with a focus on the indenter and sample holders.

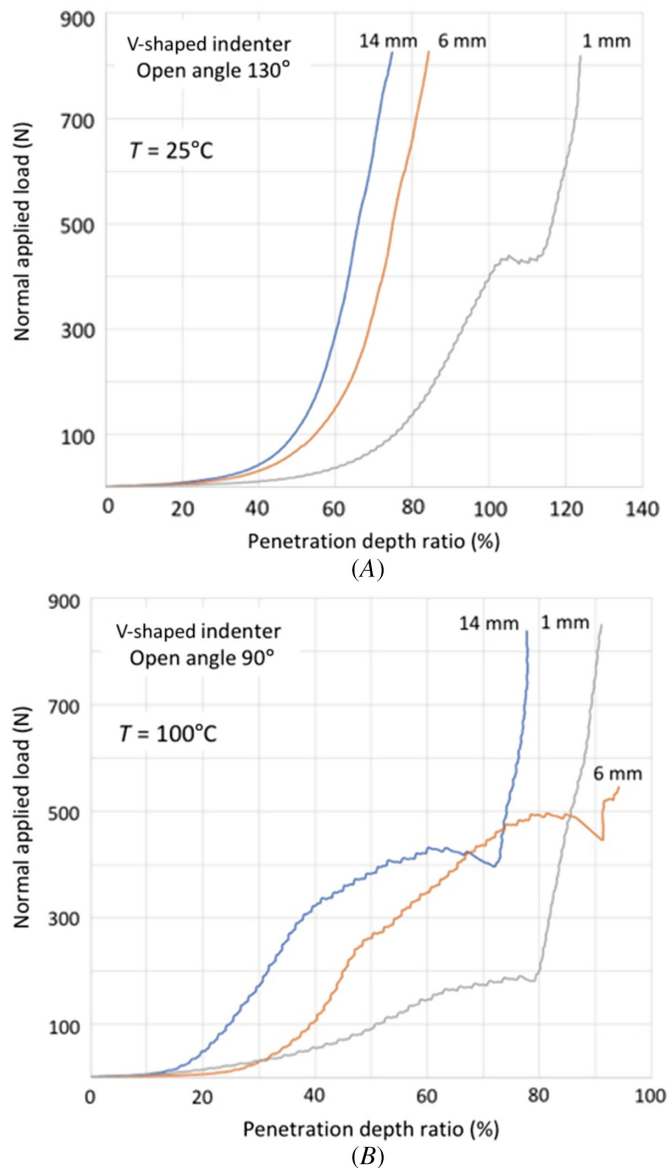


depth depending on the tip geometry (open tip angle), the slope of the curve increases in a dramatic way because 180  
of the substrate effect. At  $T = 100^{\circ}\text{C}$ , we observe a more ductile behavior with a change of the slope, with the 181  
penetration of the tip at  $F_z$ , and then the dramatic increase of the load because of the substrate effect phenomenon. 182

For a given indenter geometry, **figure 7** shows the mechanical response of the different warp yarns related 183  
to the characteristic microstructure of the grid. The resistance to penetration measured by indentation experi- 184  
ments is quite different and directly related to the resin used or the density of glass fibers embedded in resin, or 185  
both. Moreover, it is not obvious to observe that the mechanical response to the indentation experiment of warp 186  
yarns depends on the geometry of the indenter (in **fig. 7**, the edge length of V-shaped indenter; in **fig. 8**, 187

**FIG. 6**

Examples of load-displacement curves obtained at room temperature (A) and at  $T = 100^\circ\text{C}$  (B) using V-shaped indenters with different edge lengths and open tip angles.



the conical-shaped indenter) but also on the testing temperature. ESEM observations have been performed on the residual imprint left on the surface using a V-shaped indenter (fig. 9). It is interesting to note that the glass fibers are cut in a brittle way by the indenter edge. The damage generated by the indentation process propagates deeper than the near surface region. It is interesting to note that any pop-ins cannot be observed on the recorded loading curve. These pop-ins are in general related to crack formation under the tip during penetration. This phenomenon can be explained by the fact that the cutting process of individual glass fiber does not liberate much fracture energy and cannot be detected on the macroscopic load-displacement curve.

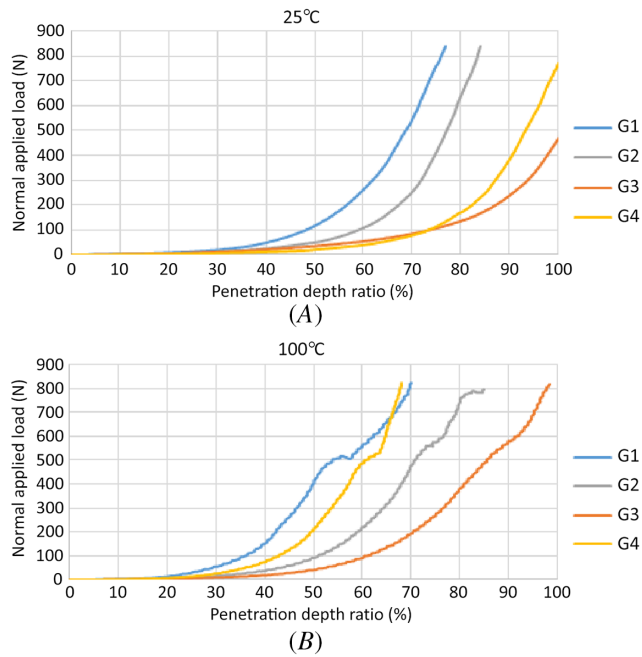
In order to reproduce effects of compaction and trafficking on the mechanical properties of geogrid damage, we have performed, using two V-shaped indenters with an aperture of  $90^\circ$  and with an edge length of 6 mm and 1 mm, respectively, one indentation in the middle of 5 new warp yarns, G1, at an elevated temperature ( $105^\circ\text{C}$ ) and



189  
190  
191  
192  
193  
194  
195  
196  
197

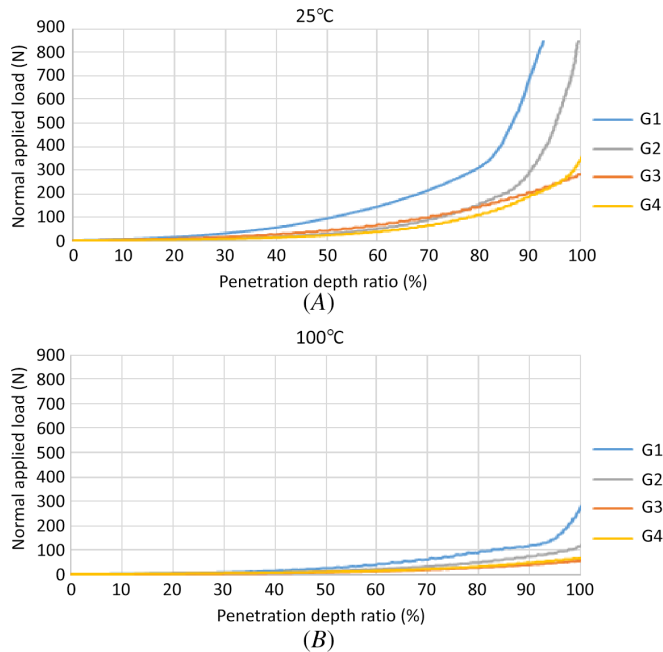
**FIG. 7**

Examples of load-displacement curves obtained on different tested grids (warp yarns) using a V-shaped indenter with a 14-mm edge length and 130° open angle at room temperature (A) and at  $T = 100^\circ$  (B).

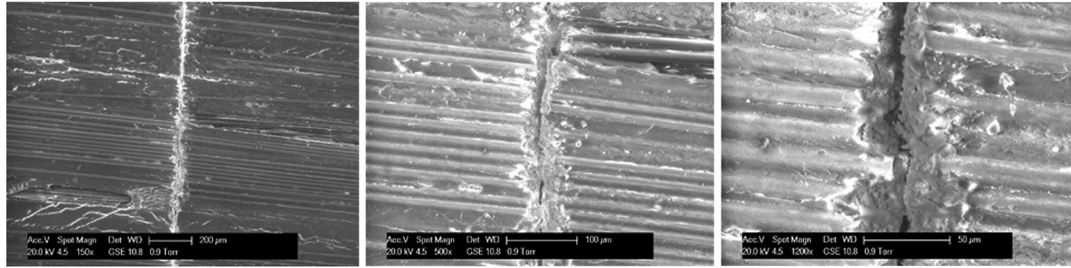


**FIG. 8**

Examples of load-displacement curves obtained on different tested grids (warp yarns) using a conical indenter with 130° open angle at room temperature (A) and at  $T = 100^\circ$  (B).



at two different pdrs (40 % and 60 % of the thickness of the new geogrid warp yarns). After this indentation, tensile 198  
 tests have been performed on these indented new geogrid warp yarns. The mechanical property results (strength 199  
 and secant modulus at the maximal strength) are presented in Table 2 for the 20 indented new warp yarns. 200

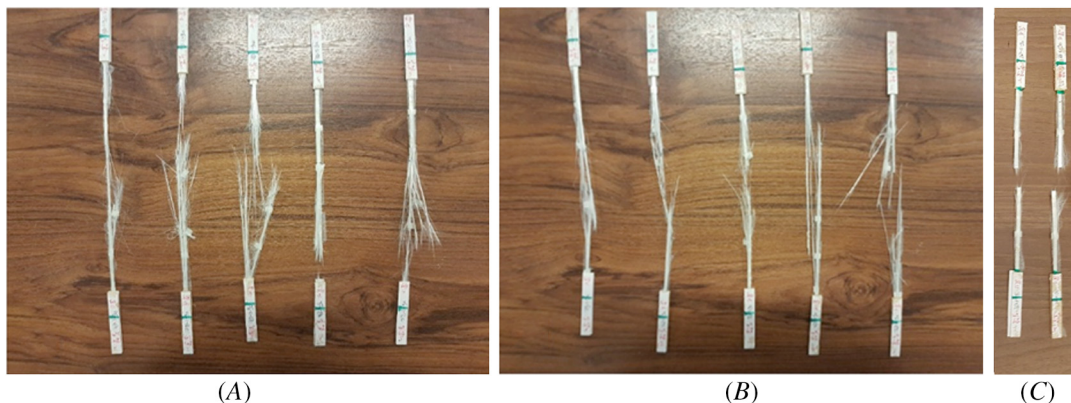
**FIG. 9** ESEM observations of residual imprint after indentation test using a V-shaped indenter geometry.

The mechanical properties are affected by the indentation effect, especially the resistance strength that is slightly reduced, as described in [Table 2](#), divided by 2 for indentation with a V-shaped indenter 3D-6-90 at 60 % of the thickness of a geogrid. With 3D-6-90 indenters and 105°C indentations, it was possible to partly reproduce the in situ residual strength, as previously mentioned, where residual strengths are varying between 20 and 55 % of initial tensile strengths, and residual secant moduli (moduli at the maximum strength) between 68 and 95 % of initial secant moduli at the maximum strength.<sup>6</sup> The edge length seems to be an important parameter. [Figure 10](#) shows residual tensile specimens after loading to rupture. Delaminations of the glass fibers ([fig. 10A](#)) with 7D-1-90 and a pdr of 40 % and brittle fracture with either a longitudinal propagation of the main crack ([fig. 10B](#)) with 7D-1-90 and a pdr of 60 % or a local rupture ([fig. 10C](#)) with 3D-6-90 and a pdr of 60 % are the three schemes of fracture under tensile loading, as observed also on the in situ recovered geogrid ([fig. 11](#)).

**TABLE 2**

Tensile strength and secant modulus after indentation tests on G1 warp yarns, as a function of the tip geometry and the imposed penetration depth (3D-6-90: V-shaped indenter with open angle of 90° and edge length of 6 mm; 7D-1-90: V-shaped indenter with open angle of 90° and edge length of 1 mm)

Indenter geometry	3D-6-90		7D-1-90	
Penetration depth ratio, %	40	60	40	60
Residual strength, %	86	45	88	73
Residual secant modulus, %	97	73	100	91

**FIG. 10** Optical observations of the residual tensile specimen after indentation and then after tension test to rupture (A) with 7D-1-90 and a pdr of 40 % (B) with 7D-1-90 and a pdr of 60 % (C) with 3D-6-90 and a pdr of 60 %.



**FIG. 11**

Optical observations of the residual tensile recovered specimen and then after tension test to rupture (A), delamination (B), local rupture (C), and (D) longitudinal propagation of the main crack.



## Conclusion

211

The indentation test results are encouraging, and the range of the residual strengths and secant moduli are in good agreement with what has been observed from 361 laboratory direct tensile tests performed on recovered in situ grids. These results prove that laboratory indentation tests whose indenter characteristics are determined from field measurement can be used to estimate the loss of mechanical performances because of in situ trafficking and the compaction process. This study shows that indentation tests can be a useful technique to characterize and to

212

213

214

215

216

evaluate the grid quality and that this characterization has a direct correlation with the in situ good performance of the glass fiber grids, which is the consequence.

The analysis of the influence of the V-shaped indenters' aperture and the influence of the conical shape for all warp and filling yarns of the grids will be the next step. A better understanding of the influence of the coating and multiple indentations on the residual strength or the stiffness modulus, or both, of the yarns is required. For that, we think that the plastic work of each indentation could be calculated. It would be helpful to determine the influence of the hardness of the coating and the indentation direction (parallel, 45° or orthogonal to the yarns), which generates more damage when the yarns are subjected to multiple indentations.

## ACKNOWLEDGMENTS

The work presented in this article was sponsored by the French National Research Agency (ANR—SolDuGri project ANR-14-CE22-0019).

## References

1. E. Graziani, G. Pasquini, G. Ferrotti, A. Virgili, and F. Canestrari, "Structural Response of Grid-Reinforced Bituminous Pavements," *Materials and Structures* 47, no. 8 (August 2014): 1391–1408. <https://doi.org/10.1617/s11527-014-0255-1>
2. S. Fallah and A. Khodaii, "Developing a Fatigue Fracture Model for Asphalt Overlay Reinforced with Geogrid," *Materials and Structures* 49, no. 5 (May 2016): 1705–1720. <https://doi.org/10.1617/s11527-015-0606-6>
3. I. Gonzalez-Torre, M. A. Calzada-Perez, A. Vega-Zamanillo, and D. Castro-Fresno, "Damage Evaluation during Installation of Geosynthetics Used in Asphalt Pavements," *Geosynthetics International* 21, no. 6 (December 2014): 377–386. <https://doi.org/10.1680/gein.14.00025>
4. J. Van Rompu, E. Godard, L. Brissaud, and E. Loison, "Procédé de renforcement d'enrobés Colgrill R : qualification des grilles en laboratoire et exemple de réalisation," *Revue Générale des Routes et de l'Aménagement* 944 (March 2017): 15–23. 
5. C. Chazallon, T. C. Nguyen, M. L. Nguyen, P. Hornych, D. Doligez, L. Brissaud, and E. Godard, "In Situ Damage Evaluation of Geogrid Used in Asphalt Concrete Pavement," in *Proceedings of the 10th International Conference on Bearing Capacity of Roads, Railways and Airfields* (London: CRC Press, 2017), 1517–1524.
6. C. Chazallon, J. Van Rompu, M. L. Nguyen, P. Hornych, D. Doligez, L. Brissaud, Y. Le Gal, and E. Godard, "Laboratory and In Situ Damage Evaluation of Geogrid Used in Asphalt Concrete Pavement" (paper presentation, *Eighth International Conference of European Asphalt Technology Association (EATA 2019)*, Granada, Spain, June 3–5, 2019.
7. *Standard Test Method for Determining Tensile Properties of Geogrids by the Single or Multi-Rib Tensile Method*, ASTM D 6637/D 6637M (West Conshohocken, PA: ASTM International, approved 2015). [https://doi.org/10.1520/D6637\\_D6637M-15](https://doi.org/10.1520/D6637_D6637M-15) 
8. *Mélanges bitumineux - Spécifications des matériaux - Partie 1 : enrobés bitumineux*, NF EN 13108-1 (Paris: Association Française de Normalisation, 2007).
9. *Bitumes et liants bitumineux - Spécifications des bitumes routiers*, NF EN 12591 (Paris: Association Française de Normalisation, 2009).
10. *Bitumes et liants bitumineux - Cadre de spécifications pour les émulsions cationiques de liants bitumineux*, NF EN 13808 (Paris: Association Française de Normalisation, 2013).
11. E. Godard, C. Chazallon, P. Hornych, A. Chabot, M. L. Nguyen, D. Doligez, and H. Pelletier, "SolDuGri Project : For Sustainable Reinforcements of Infrastructures with Glass Fiber Grids," *Revue Générale des Routes et de l'Aménagement* 949 (October 2017): 24–33.
12. M. Gharbi, M. L. Nguyen, and A. Chabot, "Wedge Splitting Characterisation of the Bond between Asphalt Layers Reinforced with Glass Fibre Grid," in *Proceedings of the 10th International Conference on Bearing Capacity of Roads, Railways and Airfields* (London: CRC Press, 2017), 1317–1324. <https://doi.org/10.1201/9781315100333> 
13. W. C. Oliver and G. M. Pharr, "An Improved Technique for Determining Hardness and Elastic Modulus Using Load and Displacement Sensing Indentation Experiments," *Journal of Materials Research* 7, no. 6 (July 1992): 1564–1583, <https://doi.org/10.1557/JMR.1992.1564>